AD_____

Award Number: W81XWH-09-1-0033

TITLE: Immunotherapy with Magentorheologic Fluids

PRINCIPAL INVESTIGATOR: William J. Murphy

CONTRACTING ORGANIZATION: UC Davis Medical Center
Dermatology Department
Sacramento, CA 95817

REPORT DATE: August 2011

TYPE OF REPORT: Annual

PREPARED FOR: U.S. Army Medical Research and Materiel Command
Fort Detrick, Maryland 21702-5012

DISTRIBUTION STATEMENT: Approved for Public Release;
Distribution Unlimited

REPORT DOCUMENTATION PAGE

Form Approved
OMB No. 0704-0188

1. REPORT DATE	2. REPORT TYPE	3. DATES COVERED
August 2011	Annual	15 May 2010 – 14 May 2011

4. TITLE AND SUBTITLE

Immunotherapy with Magentorheologic Fluids

5a. CONTRACT NUMBER

5b. GRANT NUMBER
W81XWH-09-1-0033

5c. PROGRAM ELEMENT NUMBER

6. AUTHOR(S)

William J. Murphy, Ph.D.
Cahit Evrensel, Ph.D.

E-Mail: mbouchlaka@medicine.nevada.edu

5d. PROJECT NUMBER

5e. TASK NUMBER

5f. WORK UNIT NUMBER

7. PERFORMING ORGANIZATION NAME(S) AND ADDRESS(ES)

UC Davis Medical Center
Dermatology Department
Sacramento, CA 95817

8. PERFORMING ORGANIZATION REPORT NUMBER

9. SPONSORING / MONITORING AGENCY NAME(S) AND ADDRESS(ES)
U.S. Army Medical Research and Materiel Command
Fort Detrick, Maryland 21702-5012

10. SPONSOR/MONITOR'S ACRONYM(S)

11. SPONSOR/MONITOR'S REPORT NUMBER(S)

12. DISTRIBUTION / AVAILABILITY STATEMENT
Approved for Public Release; Distribution Unlimited

13. SUPPLEMENTARY NOTES

14. ABSTRACT

Successful anti-tumor effects are weakened by removal of the tumor antigen pool (i.e. surgery) or use of cytoreductive and immunosuppressive therapies (i.e. chemotherapy and radiation). We hypothesize that mechanical disruption of the tumor in situ will augment immune responses due to antigen release. Iron particles were injected as magneto-rheological fluid (MRF) into an orthotopic primary breast cancer and followed by application of a magnetic field to exert force and shear stress on the tumor. This will result in disruption of the tumor's architecture and induction of classical "danger signals": necrotic death, release of tumor antigen with activation of a localized immune response. To promote systemic immune responses we combined MRF treatments with immunotherapy (IT) at suboptimal dosages. Tumors treated with daily application of magnetic field showed increased necrotic cell death, recruitment of activated DCs (i.e. MHC II+, CD83+) to the draining LNs with production of proinflammatory cytokines/chemokines. We then combined MRF treatment with IT to determine if systemic anti-tumor effects could be achieved. Not only have we observed suppression of tumor growth on the contralateral side treated with MRF and IT but also we saw absence of metastasis to the bone marrow of animals treated with either MRF and IT or MRF and magnetic field alone. These data suggest that MRF and magnetic field application to the primary tumor synergize with immunotherapy in disseminated cancer.

15. SUBJECT TERMS
MRF: Magneto-rehological fluid iron particles, IT: immunotherapy, necrotic death, DCs: dendritic cells, cytokines, chemokines, metastasis, breast cancer, CD40, IL2

16. SECURITY CLASSIFICATION OF:			17. LIMITATION OF ABSTRACT	18. NUMBER OF PAGES	19a. NAME OF RESPONSIBLE PERSON
a. REPORT	b. ABSTRACT	c. THIS PAGE			USAMRMC
U	U	U	UU		19b. TELEPHONE NUMBER *(include area code)*

Table of Contents

Page

INTRODUCTION:

The poor immunogenicity of human cancers has led to the exploration of means to augment immune responses and potentially "break" tolerance. However, classical means to reduce tumor burden also significantly impacts the anti-tumor immune response by killing effector cells. In our model, we propose to activate the immune system in disseminated breast cancer through the localized, in vivo generation of tumor antigens and immune activation induced by physical destruction of the tumor architecture. This was accomplished by the injection of magneto-rheological fluid (MRF) intra-tumor.

MRF is a suspension of polarized ferrous particles of size varying from hundreds of microns to a few nanometers in DPBS. In a zero-field (i.e., no magnetic field applied), the particles are arranged randomly within the fluid. Under an applied magnetic field, the particles align themselves like a chain along the lines of magnetic flux. The formation of these chains changes the MRF from a liquid into a semi-solid state. This temporary solidification will cause injury to the cell membrane, loss of tumor architecture and necrotic cell death. This will allow for tumor antigen release, generation of danger signals and immune activation. To further promote systemic immunity to tumor antigens we used MRF in combination with immunomodulating agents at suboptimal dosages to activate DCs and T cells.

Mice that received the combination of MRF injections and daily application of a magnetic field showed increased tumor death by histologoical examination, and slower tumor growth in comparison to control groups. In order to quantify cell death in the primary tumor, we used flow cytometry and stained for CD45- tubulin + 7AAD-. Tubulin negative cells are indicative of loss of cell structure and hence death by necrosis. Our data demonstrate significant tumor death by flow cytometry when mice are treated with MRF and magnets in comparison to mice treated with either PBS or MRF alone. This tumor destruction was accompanied with increased production of pro-inflammatory cytokines (IL-6) and chemokines (CCL 4 and CCL5) in the tumor site. We also observed increased recruitment of activated dendritic cells (i.e. MHC II+, CD83+) to the tumor site and the draining lymph nodes whereas this was not the case for the spleen and for the non-draining lymph nodes, suggesting a localized inflammatory response to the site of tumor.

We then applied this treatment with or without immunotherapy to determine if systemic anti-tumor effects could be attained. Tumors were inoculated on both sides of the mammary fat pad and only one tumor (direct) was treated with MRF and magnetic field followed by systemic immunotherapy. We observed suppression of tumor growth on the contralateral side only in groups receiving low doses of immunotherapy in combination with the MRF treatment. These data suggest that MRF with magnetic field application and immunotherapy can induce a systemic anti-tumor immune response and therefore may be used to target metastatic disease.

BODY:

Hypothesis and Specific Aims

This proposal is based on the hypothesis that use of shear-force destruction of the tumor in situ, without the use of cytoreductive agents, will allow and enhance immune responses due to antigen release and pro-inflammatory cytokine induction and immune cell infiltration. We have found that injection at the tumor site with biocompatible magnetic rheological fluids (MRF) (i.e. a suspension of magnetic iron micro or nanoparticles) followed by application of a magnetic field results in immediate consolidation of the particles which were dispersed into the tumor. This iron particle aggregation leads to massive destruction of the tumor architecture with tumor cell death. While modest direct anti-tumor effects using this approach alone were observed, the combination of this approach with immunotherapy resulted in significant and, importantly, systemic augmented anti-tumor responses. Thus, destruction of the tumor while preserving the antigen pool and augmentation of immune cell responses may allow for more vigorous anti-tumor responses to metastatic disease without the

need for cytoreductive therapies. This represents a novel means to use the primary tumor as an antigen source and allow its destruction while at the same resulting in immune cell activation.

We hypothesize that injection of MRF into a primary tumor followed by magnetic field application will result in the classic induction of "danger signals": necrotic tumor death, disruption of the tumor architecture and release of tumor antigens culminating with recruitment and activation of a localized immune response. Subsequent or co-administration of stimulators of dendritic cells and T cells will result in dendritic cell expansion and activation and IL2 with provide growth stimulation to $CD8^+$ T cells. Used in combination therapy with classical immunomodulating agents, this treatment will provide activation of the immune response, provide tumor antigen to dendritic cells and maintenance of cytotoxic tumor-specific T lymphocytes. These responses will result in significant systemic anti-tumor responses. To ascertain the potential efficacy and mechanisms underlying this approach we propose **two specific aims**:

<u>Specific aim 1:</u> To determine the efficacy of MRF treatment for the promotion of an anti-tumor response alone or in combination with immunotherapy.

- ✓ *Subaim 1.A. Does MRF and magnetic field application result in the induction of "danger signals" which can result in inflammatory signals and promote immune responses?*
- ✓ *Subaim 1.B. Effects of immunotherapy on MRF and magnet application followed by immunotherapy on both primary and disseminated tumors.*
- ✓ *Subaim 1.C. Assessment of the effects of MRF and magnetic field application on disseminated disease.*

<u>Specific aim 2:</u> Augmentation of immune activation using iron particles coated with anti-CD40 (ferro-immunoconjugates).

- ✓ *Subaim 2.A. Develop a biocompatible coat for MRF containing conjugated to CD40 antibody.*
- ✓ *Subaim 2.B. Determination of the biologic activity of the ferro-immunoconjugates in vitro.*
- ✓ *Subaim 2.C. Assessment of ferro-immunoconjugate activity in vivo.*

<u>Results:</u>

<u>Specific aim 1:</u> To determine the efficacy of MRF treatment for the promotion of an anti-tumor response alone or in combination with immunotherapy.

Preliminary experiments have shown that the MRF and magnet treatments were well tolerated by the mice with no obvious signs of discomfort during the period of treatment. **Figure 1** summarizes the schedule of tumor treatments. The maintenance of MRF at the site of injection was discernible by the persistence of magnetic attraction to the MRF in the tumor during a 4 day period as detected by Per's Prussian staining of iron particles at the primary tumor (**Figure 2**). Importantly, these iron particles will not be taken up by macrophages or granulocytes in the tumor due to their large size (MRF: 3-5 micron) to be phagocytozed by these immune cells. We also observed a significant inhibition of 4T1 tumor growth compared to mice that received PBS or MRF without magnetic field treatment through time (**Figure 3**). These results demonstrate that MRF can be safely injected into subcutaneous tumors, that the treatment is well tolerated and MRF and magnetic field delays tumor growth.

We next examined the effect of MRF or MRF and magnetic field application within the tumor. We have performed preliminary dosing and timing of magnet application and found that these conditions will induce significant destruction of the tumor architecture by histological examination (**Figure 4**). Furthermore, mice treated with MRF and magnet showed increased necrotic cell death and lower apoptotic cell death as illustrated in **Figure 5**. Tubulin-positive 7AAD-negative cells are the cells that have lost integrity of the cell membrane due to the shear force of the MRF and magnet application and therefore are considered necrotic cells (1, 2). All Tubulin+ 7AAD+ cells are in the apoptotic stage.

From these results, we suggest that this approach can cause disruption of the tumor architecture, tumor cell death by necrosis, and release of tumor antigen. All these are attributes of "danger signals". However, remaining issues to be investigated is the determination of the appropriate magnetic field strength and distribution as well as exploring the size of the iron particle.

Once we have determined the efficacy of magnetic field application and MRF, we then used this protocol as an adjuvant with immunotherapy. Immunotherapeutic regimens have focused on means to elicit and promote T cell responses and the use of MRF/FF and magnetic field application may further augment the efficacy of these approaches due to not only induction of "danger signals" but also tumor antigen release. We have previously shown that agonist anti-CD40 and recombinant human-IL-2 therapy results in synergistic and significant anti-tumor responses against metastatic disease in advanced tumor bearing mice (3). Augmentation of these responses may be possible if greater tumor antigen exposure is followed by DC recruitment and activation locally. Therefore, we performed preliminary experiments to determine if MRF and magnet treatment would augment anti-tumor responses in combination with anti-CD40 and IL-2 treatment. Mice received 4T1 on both sides of the mammary fat pad. Only the ispilateral (primary) tumor received intratumoral injection of MRF or PBS as a control. One day following MRF or PBS implantation, magnet treatment is initiated on the ispilateral tumor for a total of 5 treatments. In combination with magnet treatments one group received a suboptimal dose of anti-CD40 (25 ug/dose, 1 injection a day for 5 days) and recombinant human IL2 (2.5 $x10^5$ IU/dose, 1 injection a day on days 1, 4 and 8 post MRF injection) intraperitoneal as to measure any augmentation of response with MRF and magnet field. An additional group received immunotherapy alone without MRF treatments. Schema and schedule of treatment is illustrated in **Figure 6.**

Preliminary data indicates that even greater disseminated effects can indeed be obtained (**Figure 7**) with the multiple approach therapy. We saw slower growth of the contralateral tumor after MRF and magnet treatment on the primary tumor. Most importantly these anti-tumor responses are increased when combined with a suboptimal dose of anti-CD40 and IL2 which when administered alone has similar effects to PBS treated animals (**Figure 7**). Because we have previously demonstrated anti-tumor effects after combination of anti-CD40 and IL2 in a model of metastatic renal carcinoma (3), we wanted to determine the effects of MRF and magnetic field on disseminated disease. BALB/c mice received 4T1 on one side of the mammary fat pad as described earlier in **Figure 1**. At the end of MRF and magnet treatment, tumor colony forming units (CFU) in the bones were determined. To our surprise, metastasis to the bones of MRF and magnet treated group were almost nonexistent. As expected, PBS or MRF alone had no effect on metastasis of primary tumors. Therefore, MRF and magnet may either inhibit primary tumors to metastasize or have other effects on disseminated disease itself (**Figure 8**).

We next determined the effector population in the tumor responses after MRF implantation and magnetic field treatment as we have previously shown that increases in both DCs and $CD8^+$ T cells occur after anti-CD40 and IL2 therapy (3), demonstrating that they may play a role in the immune response to the tumors. Indeed, we have observed an expansion of mature $CD11c^+$I-A^+ CD83+ DCs in the draining LNs and tumor of 4T1 tumor bearing mice only in the group treated with MRF and magnetic field both in total frequency (not shown) as well as in numbers (**Figure 9**). DC recruitment was specific to the tumor and draining LNs as opposed to the spleen and non-draining LNs. These data suggest that MRF treatment induced a localized immune response.

The increased frequency of mature DCs in the tumor after MRF treatments was accompanied with an increase in secretion of inflammatory cytokines and chemokines at the tumor site determined by qPCR (**Figure 10**). The histological and immunohistological assessments will thus be pivotal to determine mechanisms of action. It will also be important to determine T cell cytokines and subsets at the site and regional lymph nodes. Recently IL17 producing cells have been shown to dominate in inflammatory states which may limit or hamper productive Th1 responses. Therefore, cytokine profiles for future studies will be determined in tissues and serum by qPCR and Luminex, respectively, looking at IL-2, IFNγ, IL-1 IL-12, IL-10, IL-4 and IL-17. These cytokines are being assessed in current experiments.

Specific aim 2: Augmentation of immune activation using iron particles coated with anti-CD40 (ferro-immunoconjugates).

In the parent award grant, we have proposed to coat the iron particles with an agonist anti-CD40 in order to administer the immunotherapy locally intratumor. Mobilization of anti-CD40 instead of its systemic administration offers the following advantages: 1) clearance of the antibody should be reduced, 2) greater localization at the tumor site should be attained, and 3) more potent immunostimulatory effects should be attained. This may allow for less systemic administration of anti-CD40 and IL2 to be needed, if at all. Several steps prior to the conjugation of anti-CD40 to the iron particles had to be done:

1) Coating of the iron particles with various polymers
2) Conjugation of surface coated polymers with fluorescent labeled albumin or antibody as a stimulant for anti-CD40.

Surface grafting of polymers on iron particles

The procedure for surface coating iron particles using various polymers via ATRP were as follows: iron particles were washed with distilled water and ethanol respectively. Then, they were dried in a vacuum oven at 50 ^{o}C overnight and cooled down. CTCS was immobilized on the surface of the iron particles at 85 ^{o}C for 24 hours under nitrogen with toluene as a solvent. The mixture was then filtered and washed with methanol in order to remove excess CTCS. The residual (Fe-CTCS) was dried in a vacuum oven at 40-50°C for 24 hours. Functionalized Fe-CTCS was then reacted with CuBr, $CuBr_2$, Spartein, and monomers in organic solvent at 25–30 ^{o}C for 24 hours under nitrogen. Finally, the mixture was filtered, washed several times with ethanol and dried in a vacuum oven at 40-50°C prior to use (4). The ATRP mechanism for surface polymerization is shown in **Figure 11**.

Conjugation of surface modified iron particles with fluorescent labeled albumin or antibody

The surface coated poly(AA) and poly(NIPAAm-co-AA) has been conjugated with fluorescent labeled albumin or antibody. The procedures of conjugation were as follows: surface coated iron particles were washed with Polylink conjugation buffer (50mM MES, pH 5.2, 0.05% Proclin-300) and mixed for 1–2 minutes. Then, iron particles were separated using a magnet for 3 minutes and the supernatant was removed. The iron particles were re-suspended in a conjugation buffer (MES buffer) and mixed for 1–2 minutes. The EDAC solution (200mg/mL) was added to the iron particle suspension and mixed for 1–2 minutes. Fluorescent labeled albumin or antibody was then added to the suspension and incubated for 1 hour at room temperature. The un-conjugated fluorescent labeled albumin or antibody was washed several times using washing buffer (10mM Tris, pH 8.0, 0.05% Bovine Serum Albumin, 0.05% Proclin-300) by separating iron particle using magnet and removing supernatant. The iron particles were stored in wash buffer prior to characterization. The conjugation mechanism of fluorescent labeled albumin or antibody and modified iron particles through poly(AA), and poly(NIPAAm–co–AA) are shown in **Figure 12**.

Conjugation of carboxylic acid functionalized microsphere with fluorescent labeled albumin as a benchmark

The Polylink protein coupling kit consist of functionalized carboxylic acid–iron microparticles, MES buffer solution, and wash/storage buffer, was warmed slightly above room temperature (5). Then, iron particles were separated using magnet for 3 minutes an the supernatant was removed. The iron particles were re-suspended in conjugation buffer (MES buffer) and mixed for 1–2 minutes. These steps were repeated twice. The EDAC solution (200mg/mL) was added to the iron particle suspension and mixed for 1–2 minutes. Fluorescent labeled albumin or antibody was then added to the suspension and incubated for 1 hour at room temperature. The un-conjugated fluorescent labeled albumin or antibody was washed several times using washing buffer (10mM Tris, pH 8.0, 0.05% Bovine Serum Albumin, 0.05% Proclin-300) by separating the iron particles using a magnet and removing supernatant. The iron particles were stored in wash buffer prior to characterization. The conjugation mechanism of carboxylic acid functionalized microsphere with protein is shown in **Figure 13**.

Characterization

The non- and coated iron particles were characterized using scanning electron microscopy (SEM). The thermal properties of the surface grafted polymers on the iron particles were characterized using Perkin-Elmer Pyris-1 differential scanning calorimetry (DSC). The surface grafted polymers/iron particles were dried in a vacuum oven at 60^{o}C for 24 hours and were stored in a desiccator prior to characterization. Each sample was placed in the sample pan and scanned from 25 ^{o}C to 300 ^{o}C with a heating rate of 10 ^{o}C/min, under high purity nitrogen purge with a volumetric flow rate of 20 ml/min. The conjugated fluorescent labeled protein or antibody on the surface grafted polymers of iron particles was characterized using flow cytometry.

The presence of polymer on the surface of iron particles and the thermal transition temperature of the grafted polymers has been analyzed using differential scanning calorimetry (DSC). A change of heat supplied (heat flow endo up – Y-axis) signifies the individual thermal transition temperature of each polymer. The glass transition temperature of polymer grafted onto the surface of iron particles was measured in the experiments. Then, the thermal transition temperatures from experiments were compared with available data from the literature which has been found for non-grafted polymers. The decreased mobility of the polymer due to the covalent bonding on the surface of the iron particles may result in the differences in glass transition temperatures between literature and experiment. The results were in agreement with literature (6) which compared the thermal transition temperature between polystyrene and grafted polystyrene onto the surface of silica oxide. The literature value was approximately 20 ^{o}C higher for the grafted polymer. The glass transition temperature of a variety of polymers is shown in Table 1 and the DSC results for several polymers are shown in **Figure 14.** The SEM images of non- and coated iron particles are shown in **Figure 15**.

The anti CD40 antibody was substituted with commercially available fluorescein (FITC)-conjugated ChromPure Rat IgG and fluorescinated albumin for preliminary experiments. The fluorescinated albumin and fluorescein (FITC)-conjugated ChromPure Rat IgG have been successfully conjugated on the surface of iron particles through a covalent bond on the polymer backbone. These were shown from the result of flow cytometry test. From the cytometry test, the distribution of unlabeled (control) surface modified iron particles is shown on the left side of graph. On the right side of **Figure 16** (a), (b), (c), and (d) represented the conjugated either fluorescein (FITC)-conjugated ChromPure Rat IgG or fluorescinated albumin onto surface modified iron particles. Figure 13 (a) represented the iron particles modified with poly(AA)– fluorescein (FITC)-conjugated ChromPure Rat IgG. It can be seen that the distribution of particles shifted to the right which representing the presence of fluorescent marker on the iron particles. Similarly, the shifting particles distribution was also occurs for Figure 13 (b) iron modified with poly(AA)–fluorescent labeled albumin, Figure 13 (c) iron modified with poly(NIPAAm-co-AA)–fluorescein (FITC)-conjugated ChromPure Rat IgG, and Figure 13 (d) commercially available Polylink protein coupling kit consists of functionalized carboxylic acid–iron microparticles with fluorescent labeled albumin which has been used for a benchmark. The particles distribution on Figure 13 (b) has not been shifted significantly because the amount of carboxylic acid group, which is reactive functional group to conjugate with albumin or antibody, was less since this system was copolymer of NIPAAm and carboxylic acid.

Determination of the biologic activity of the ferro-immunoconjugates in vitro

After conjugation of anti-CD40 with fluorescein (FITC) albumin to the iron particles (described in **Figure 16**), we conducted some in vitro tests to determine if the CD40-ferro-immunoconjugates were able to stimulate DC proliferation. Whole splenocytes from Balb/c mice were harvested and brought into cell suspension then stimulated with two positive controls: with lipopolysaccharide (LPS) or with unconjugated anti-CD40 and finally compared to the conjugated-CD40-immunoconjugated as illustrated in **Figure 17**. Serial diultions of LPS, anti-CD40 or iron-CD40 were performed or no stimulation of splenocytes. Cells were incubated at 37 degrees Celsius for 4 days, then pulsed with Thymidine [^{3}H] for 16-18 hours and thymidine incorporation was assessed on a Wallac- scintillation counter. Unfortunately as shown in **Figure 17**, the conjugated iron-CD40 particles were unable to induce cell proliferation as opposed to unconjugated anti-CD40 (free CD40) or LPS stimulation which could be possibly due to inappropriate conformational conjugation of the antibody to the iron particles. In the future we would like to pursue conjugation of other molecules such as CpG which also can activate DCs and possibly be used as an alternative to anti-CD40.

KEY RESEARCH ACCOMPLISHMENTS:

1. Localization of iron particles to the primary tumor without toxicity from the iron particles and magnet treatments observed.
2. Slower tumor growth of orthotopic primary breast carcinoma (4T1).
3. Increased necrosis and decreased apoptosis of primary tumor after MRF and magnetic field application.
4. A significant increase in the frequency and the total number of activated dendritic cells (MHC II+ CD83+) in the tumor and draining L.N as opposed to the spleen. These data suggest that the therapy induced a localized immune response.
5. Induction of pro-inflammatory cytokines (IL-6) and chemokines (CCL3, CCL4 and CCL5) important for activation of the innate and adaptive immune system.
6. A significant inhibition of untreated contralateral tumor with synergistic effect when MRF and magnet treatments (primary tumor) are combined with suboptimal dose of immunotherapy.
7. Systemic anti-tumor effects by inhibition of metastasis of murine breast cancer to the bones after MRF and magnet treatment or in combination with low dose of immunotherapy.
8. This suggests that MRF with magnetic field can be used to target disseminated disease and possibly be combined with immunotherapy.
9. Minimal toxicity observed when MRF and magnet were combined with suboptimal dosages of anti-CD40/IL2 systemic administration.
10. Various polymers, such as: poly(NIPAAm), poly(AA), and poly(NIPAAm-co-AA), have been grafted onto the surface of iron particles in order to provide functionalities of MRF.
11. As compared with synthesized bulk polymer, the thermal transition temperatures of grafted polymers were higher due to covalent bonding of the polymer to the surface of the iron particles.
12. For preliminary experiments of conjugation antibody onto iron particles, anti-CD40 has been simulated using commercially available fluorescein (FITC)-conjugated ChromPure Rat IgG and fluorescinated albumin. The fluorescent marker and conjugated antibody attached to the iron particles was successfully identified using flow cytometry.
13. Although, from the flow cytometry data the conjugation of anti-CD40 to the iron particles seemed to be successful, their ability to stimulate spleen cells in vitro were unsuccessful as they failed to induce cell proliferation and this could be possible due to inappropriate orientation of the CD40 conjugation to the iron particles.

REPORTABLE OUTCOMES:

- Manuscript in preparation as we had to move our laboratory a second time at the UC Davis Medical Center to a different location from Research III building to the Institute for Regenerative Cures (IRC)

building. We moved in September 2010 and therefore we had to repeat the same experiments in order to make sure that data repeats.

- Published abstracts for funding period of current Award (2008-2010):

  - Myriam **Bouchlaka**, Danice Wilkins, Alan Fuchs, Cahit Evrensel, and William Murphy. **"**Mechanical disruption of the primary tumor using magnetic beads inhibits metastasis of breast cancer"**.** J. Immunol., Apr 2010; **184**: 100.24.

  - **Bouchlaka MN**, Fuchs A, Evrensel CA, Welniak LA, Murphy WJ. Mechanical Disruption of the "Primary Tumor Using Biocompatible magnetic Beads in Combination With Immunotherapy Allows for Systemic Anti-tumor Responses in Metastatic Breast Cancer". J Immunother. 31: 939, 2008.

CONCLUSIONS:

Successful anti-tumor effects are weakened by removal of the tumor antigen pool (i.e. surgery) or use of cytoreductive and immunosuppressive therapies (i.e. chemotherapy and radiation). We hypothesize that mechanical disruption of the tumor in situ will augment immune responses due to antigen release. Iron particles were injected as magneto-rheological fluid (MRF) into an orthotopic primary breast cancer and followed by application of a magnetic field to exert force and shear stress on the tumor. We have demonstrated that injection of a 60% w/v solution of 3-5 micron carbonyl iron particles (MRF) into othotopic 4T1 tumors followed by exposure to a strong (0.4 Tesla) magnetic field resulted in tumor destruction, as judged by tumor shrinkage and tumor necrosis as judged by flowcytometry, as well as induction of a local inflammatory response, as evidenced by mRNA for several proinflammatory cytokines and recruitment of mature DCs (i.e. MHC II+, CD83+) to tumors and draining LNs, as judged by flow cytometry. Most importantly, no signs of toxicity has been observed during and post MRF and magnet treatments. These data support our hypothesis that disruption of the tumor's architecture and induction of classical "danger signals": necrotic death, release of tumor antigen with activation of a localized immune response.
To promote systemic immune responses we combined MRF treatments with immunotherapy at suboptimal dosages. Not only have we observed suppression of tumor growth on the contralateral side treated with MRF and IT but also we saw absence of metastasis to the bone marrow of animals treated with either MRF and IT or MRF and magnetic field alone. These data suggest that MRF and magnetic field application to the primary tumor synergize with immunotherapy in disseminated cancer.

Unfortunately, we have been unsuccessful at coating the iron particles with an agonist mAb to CD40. Generation of ferro-immunoconjugates was part of Aim2 of the parent award in which we hypothesize that greater immune activation would occur by administering agents that induce DC activation (i.e: agonist anti-CD40) at the tumor site such that greater antigen-uptake and presentation can occur there and in the draining lymph nodes. To circumvent this problem we are currently testing the conjugation of CpGs with the iron particles. CpGs have been recently demonstrated to activate DCs and to overcome tumor-mediated suppression pathways that occur within the tumor (4-7). Therefore, CpG conjugates will replace the anti-CD40, this work is in progress.

REFERENCES:

1. O'Brien MC, and Bolton WE: Comparison of cell viability probes compatible with fixation and permeabilization for combined surface and intracellular staining in flow cytometry. *Cytometry*. 19(3), 243-255 (1995).
2. O'Brien MC, Healy SF, Jr., Raney SR, *et al.*: Discrimination of late apoptotic/necrotic cells (type III) by flow cytometry in solid tumors. *Cytometry*. 28(1), 81-89 (1997).

3. Murphy WJ, Welniak L, Back T, *et al.*: Synergistic anti-tumor responses after administration of agonistic antibodies to CD40 and IL-2: coordination of dendritic and CD8+ cell responses. *J Immunol*. 170(5), 2727-2733 (2003).
4. Vicari AP, Chiodoni C, Vaure C, *et al.*: Reversal of tumor-induced dendritic cell paralysis by CpG immunostimulatory oligonucleotide and anti-interleukin 10 receptor antibody. *J Exp Med*. 196(4), 541-549 (2002).
5. Mellor AL, Baban B, Chandler PR, Manlapat A, Kahler DJ, and Munn DH: Cutting edge: CpG oligonucleotides induce splenic CD19+ dendritic cells to acquire potent indoleamine 2,3-dioxygenase-dependent T cell regulatory functions via IFN Type 1 signaling. *J Immunol*. 175(9), 5601-5605 (2005).
6. Wu A, Oh S, Gharagozlou S, *et al.*: In vivo vaccination with tumor cell lysate plus CpG oligodeoxynucleotides eradicates murine glioblastoma. *J Immunother*. 30(8), 789-797 (2007).
7. Zhang Y, Wakita D, Chamoto K, *et al.*: Th1 cell adjuvant therapy combined with tumor vaccination: a novel strategy for promoting CTL responses while avoiding the accumulation of Tregs. *Int Immunol*. 19(2), 151-161 (2007).

APPENDICES: None

SUPPORTING DATA:

Figure 1: Schedule of tumor injections and MRF and magnet treatments.

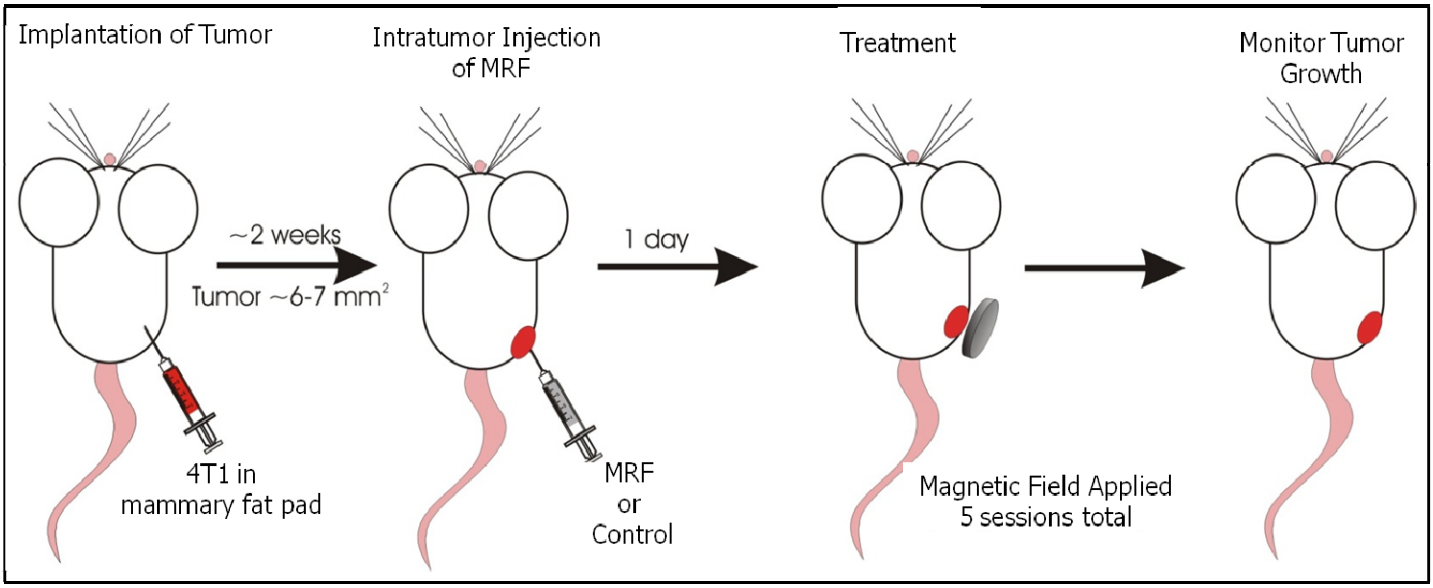

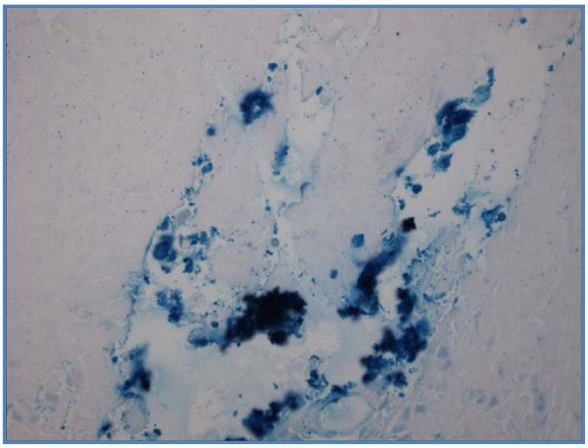

Figure 2: Localization of iron particles to tumor site. 4T1cells were injected s.c into the mammary fat pad of female BALB/c mice as described in Fig 1. About 14 days post tumor inoculation, 100 µl of 60% MRF w/v in PBS was injected into the tumor. One group was treated for 5 min with a 0.5 Tesla magnet starting 24 hours after MRF injection for 5 consecutive days. Tumor were collected on day 5 of magnet treatment and fixed on formalin. All sections were stained with Perls' Prussian stain for detection of ferrous particles. Original magnification 40X.

Figure 3: Inhibition of tumor growth with MRF implantation and magnetic field treatment. 4T1 cells were injected s.c into the mammary fat pad of BALB/c mice as shown in Fig 1. Mice received 60% w/v MRF in 100 µl PBS or PBS alone. One group was treated 24 hours after MRF injection (day 17) by placing a 0.5 Tesla magnet over the tumor for 5 min. a day for 5 consecutive days (days 18 to 22). Statistics done by Two- Way ANOVA, &: $P<0.05$ vs PBS and $P<0.001$ vs MRF, #: $P<0.05$ vs MRF, ^: $P<0.01$ vs PBS and $P<0.001$ vs MRF, *: $P<0.01$ vs PBS and $P<0.001$ vs MRF. n= 9.

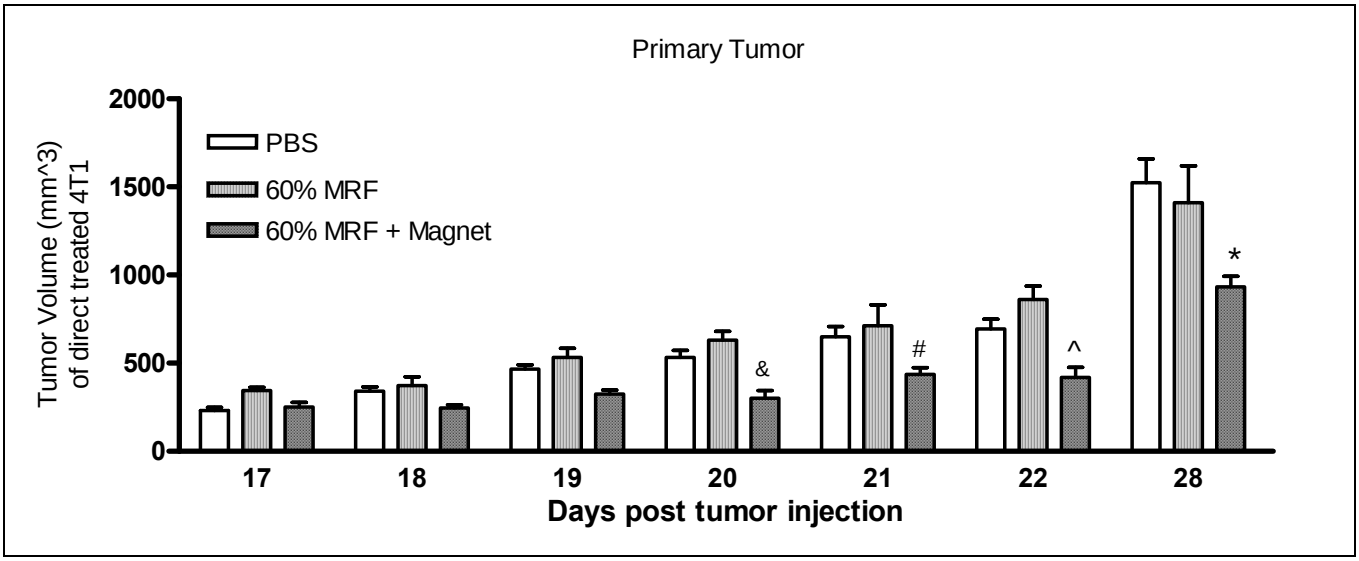

Figure 4: Histological examination of tumor at site of MRF injection. 4T1 tumors were established and treated as described in figure 1. At the end of MRF and magnet treatment, all tumor sections were fixed in formalin and stained with Hematoxylin & Eosin. Original magnification 400x. Images were captured with an Olympus BX4 microscope equipped with a Q-color3 camera and 10x numerical aperture objective lens. (a) PBS treated group. (b) MRF treated group. (c) MRF+ Magnet treated group. * represent iron particles, arrows represent infiltration of PMNs and some lymphocytes and # represent tumor cells. n = 3 mice/group.

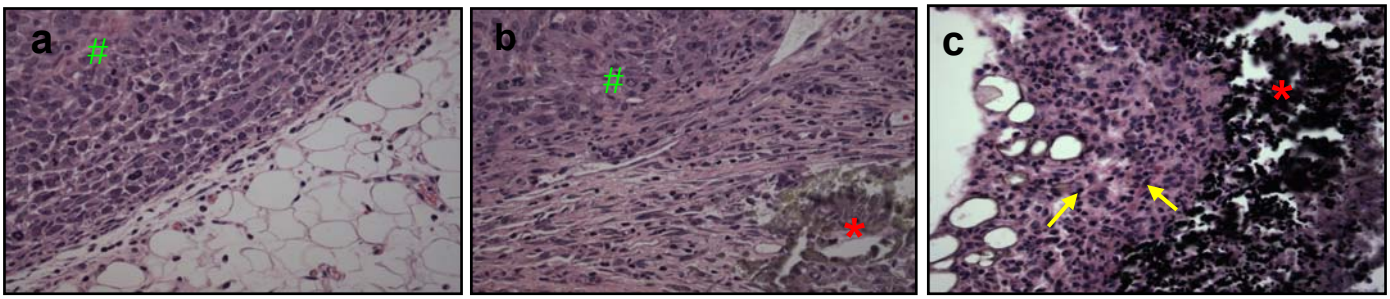

Figure 5: Increased necrosis and decreased apoptosis of primary tumors with MRF and magnet treatment. 4T1 tumors were established in Balb/c mice and treated as described in figure 1. At the end of MRF treatment, tumors were harvested and analyzed by flow cytometry for 7AAD and Tubulin expression on CD45negative cells. (A) Representative dot flow cytometry plots. MRF and magnetic field treatment results in increased necrotic death (7AAD- Tubulin+) and lower apoptotic death (7AAD+ Tubulin+). (A) apoptotic tumor death, 7AAD+ Tubulin + and (B) necrotic tumor death, 7AAD- Tubluin+. One-way ANOVA statistics. n = 3 mice/group.

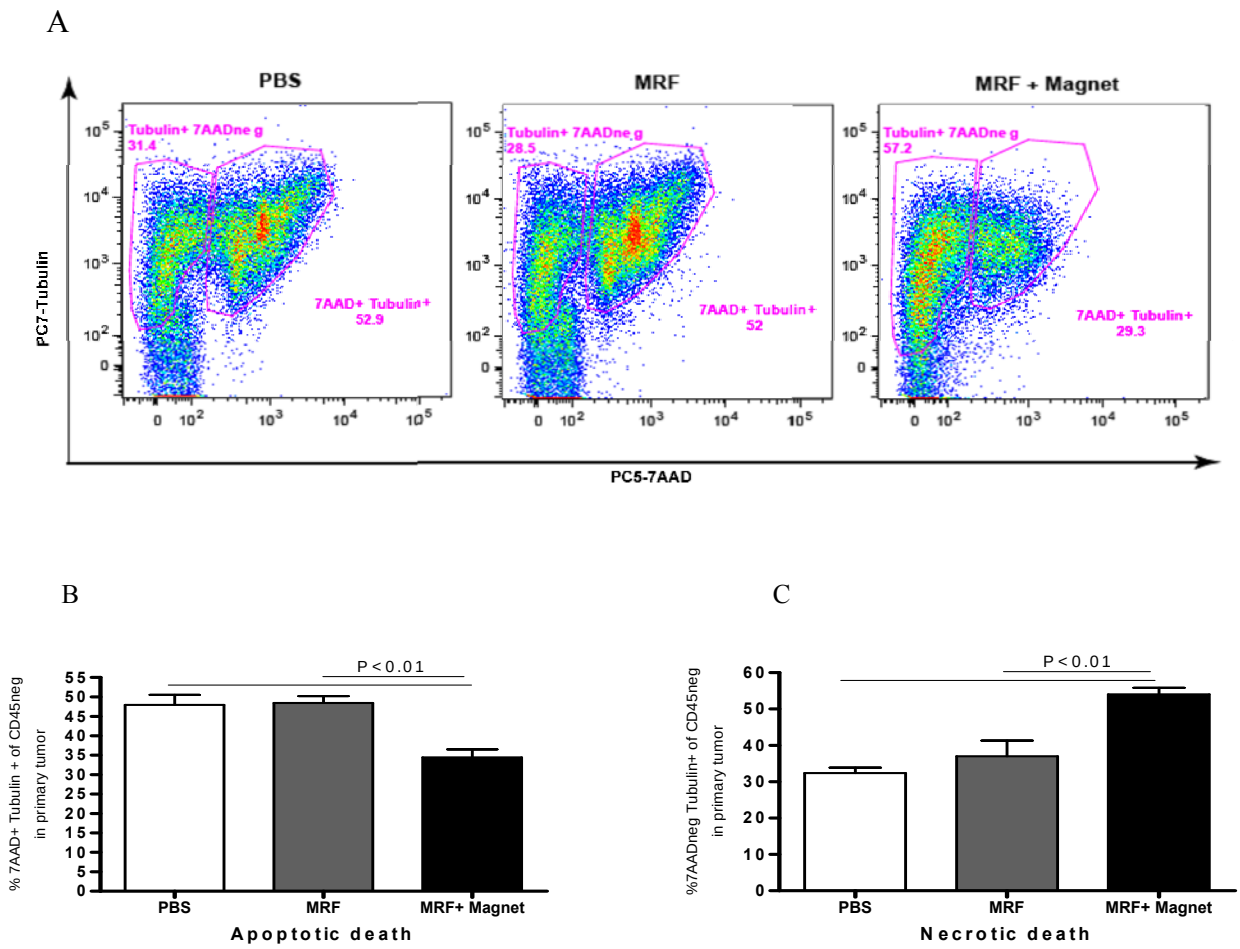

Figure 6: Model for assessment of anti-tumor effects of MRF and magnet treatment on disseminated disease.

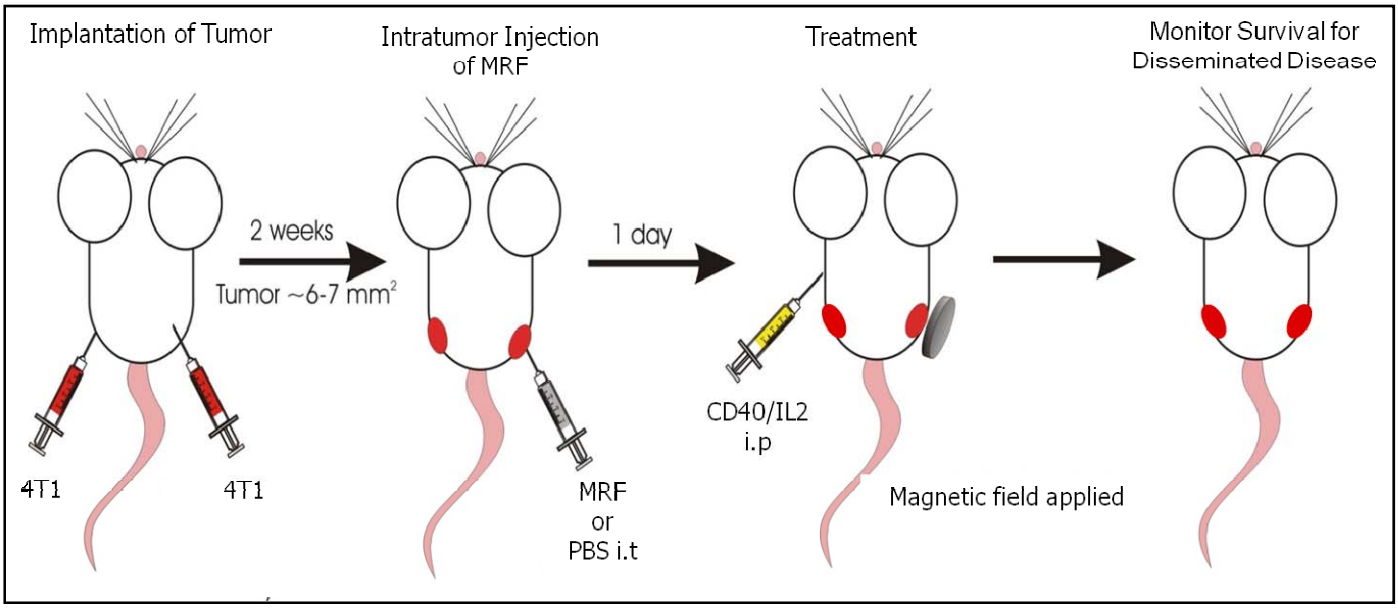

Figure 7: MRF and magnet treatment results in systemic anti-tumor effects on tumor growth. 4TI breast cancer cells were implanted on the right and left side of the mammary fat pad of BALB/c mice. Treatment was initiated two weeks post tumor injections. Only the right tumors were injected with MRF in 100 µl PBS or PBS alone. The following day, some groups were treated by placing a 0.4 Tesla magnet over the right tumor for 5 min for 5 consecutive days. Other groups received anti-CD40 (i.p) for 5 consecutive days (14 to 18 post tumor injections) at the same time of magnet treatment and rhIL-2 (i.p) on days 15, 18 and 22 post tumor injections. Tumor volumes were recorded during and after the end of treatment. Day 28 post tumor injection is shown. Two-way ANOVA statistics. n= 9 mice/group.

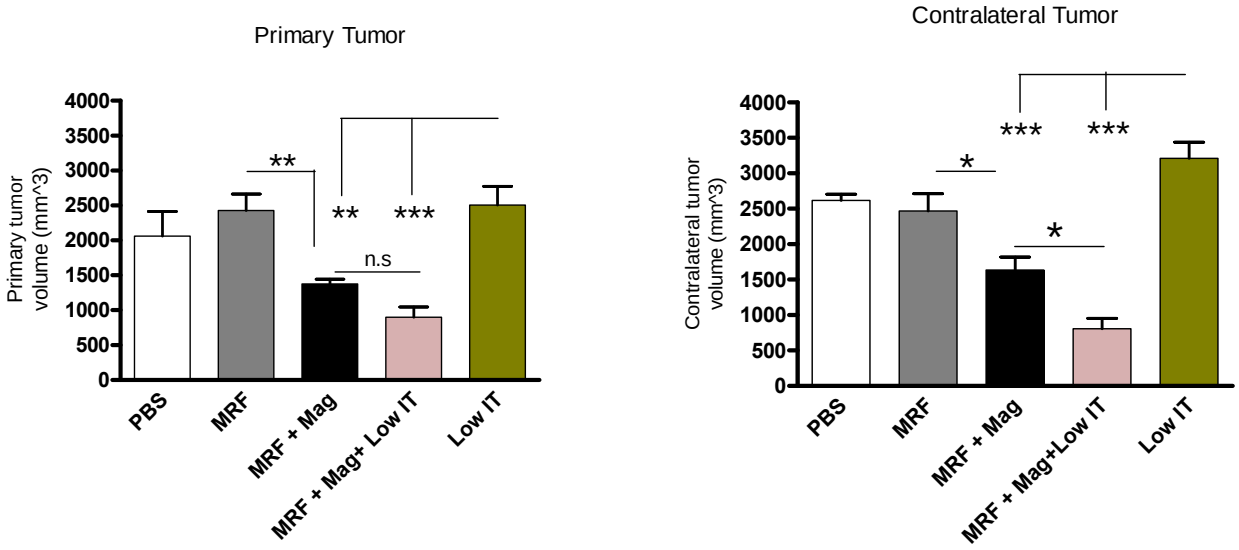

Figure 8: Inhibition of metastasis following MRF and magnet treatment. On day 26 post tumor injections, femurs of mice were harvested. For tumor colony-forming-units (CFU) assay, BM cells were cultured and incubated for 14 days and tumor colonies counted. *P<0.001. n=3.

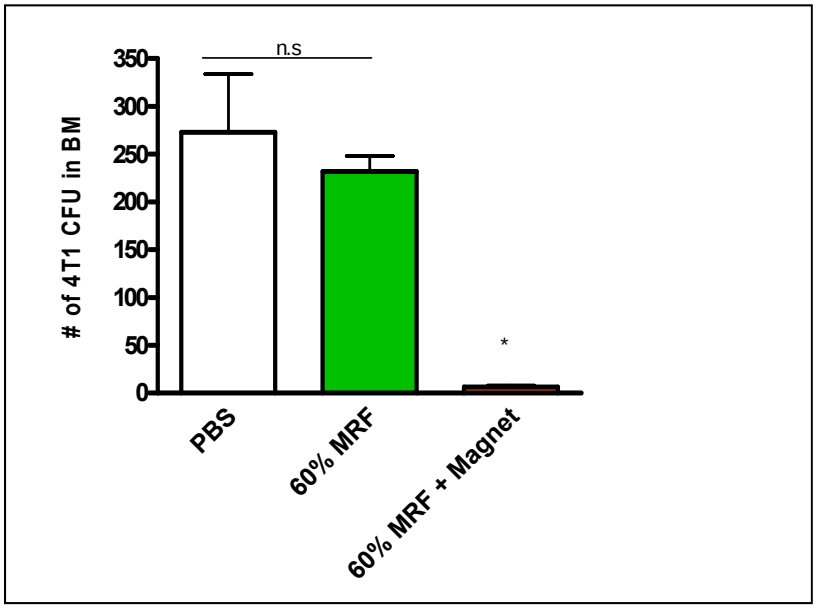

Figure 9: Increased total numbers of activated dendritic cells in the tumor and draining lymph node after MRF and magnet treatment. Tumors were established and treated as described in Fig 1. Spleen, tumor, non-draining L.N and DL.N were analyzed by flow cytometry for CD83, MHC II, and CD11c+ of CD45+ cells. One-way ANOVA statistics, n= 3-4. One-Way ANOVA statistics.

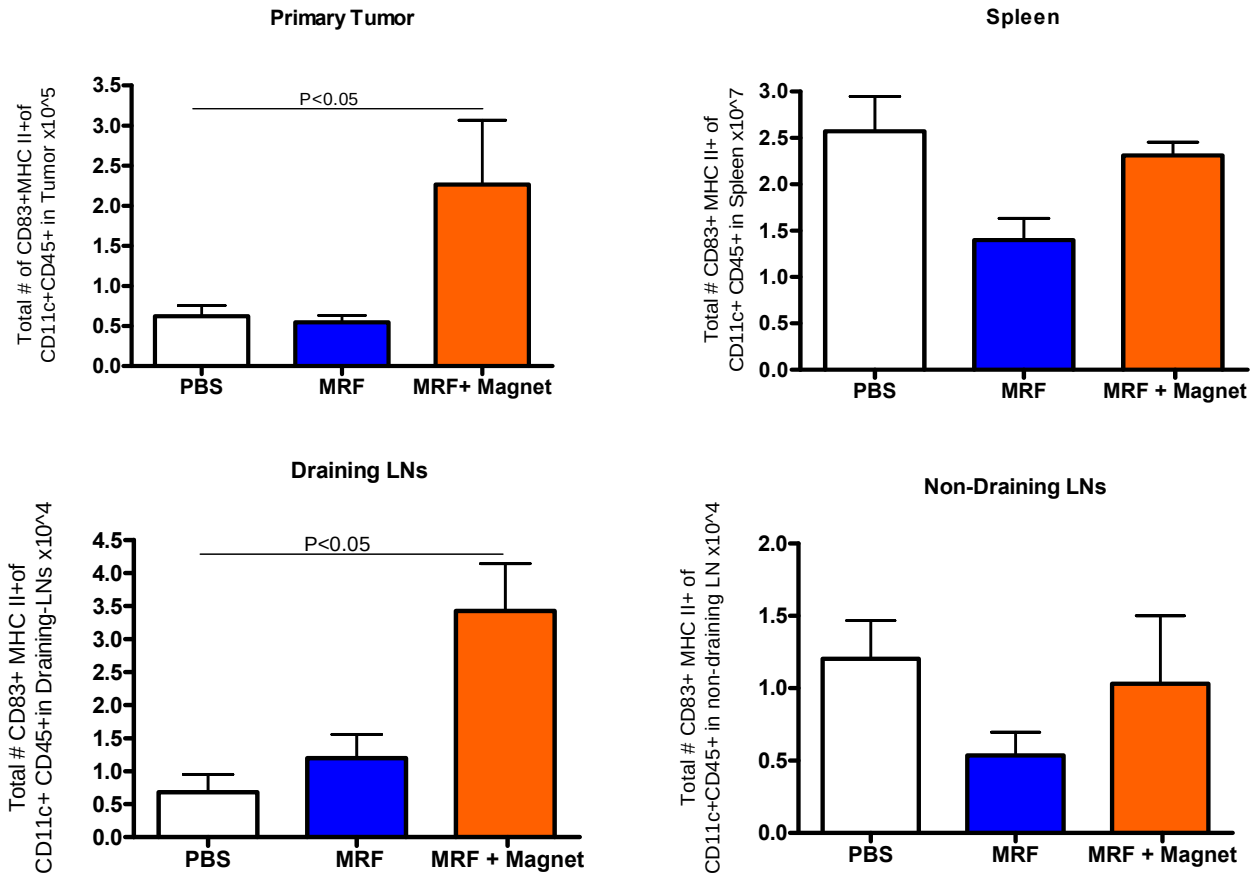

Figure 10. Increased proinflammatory cytokine and chemokine gene expression in tumors. Tumors were established and treated as described in Fig 1. mRNA expression was determined by qPCR. Results were normalized to HPRT1 and expressed as ΔΔCt in which the changes in gene expression untreated tumors (ΔCt) are compared to the mean value for the ΔCt in PBS treated tumors.

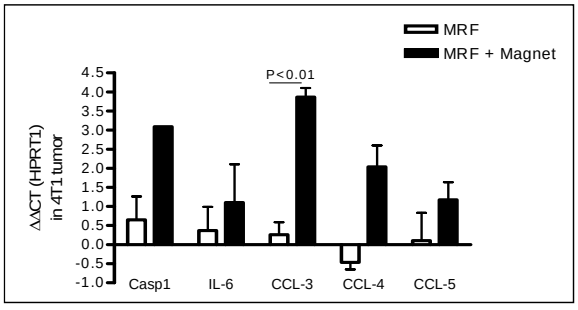

Figure 11: Surface polymerization of various polymers: poly(NIPAAm), poly(AA), and poly(NIPAAm-co AA) on the iron particles using ATRP technique.

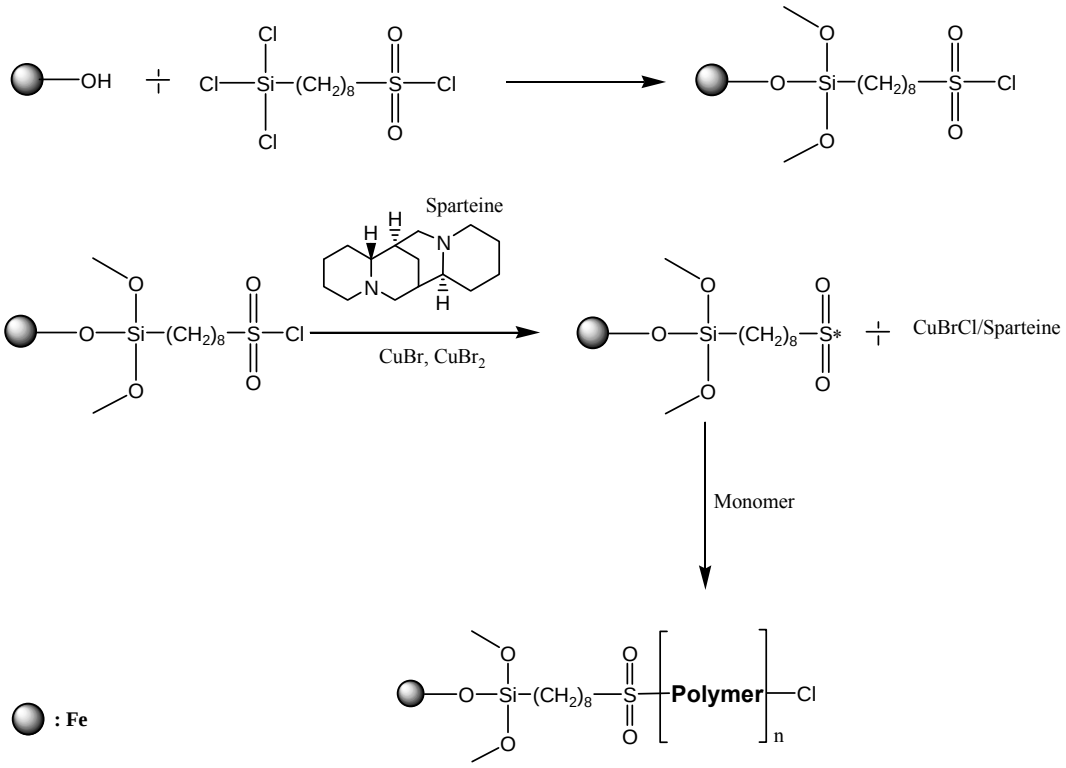

Polymer: **Poly(NIPAAm)** **Poly(AA)** **Poly(NIPAAm-co-AA)**

Figure 12: Conjugation of fluorescent labeled albumin or antibody and modified iron particles through (A) poly(AA), and (B) poly(NIPAAm–co–AA) (7, 8).

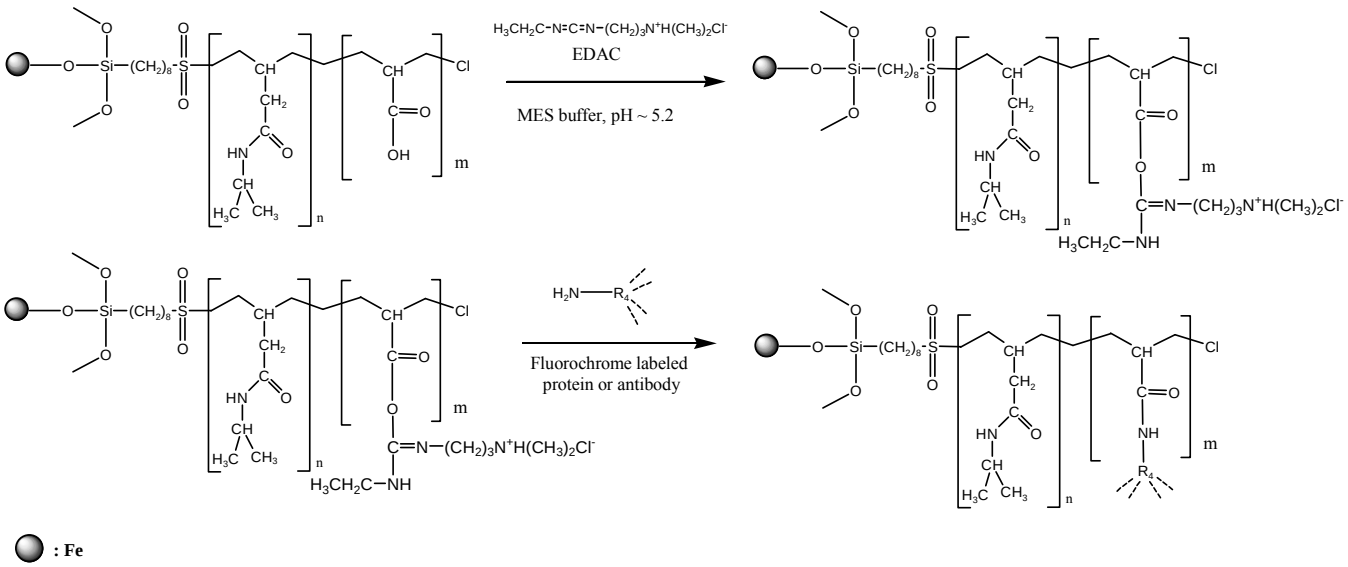

(A)

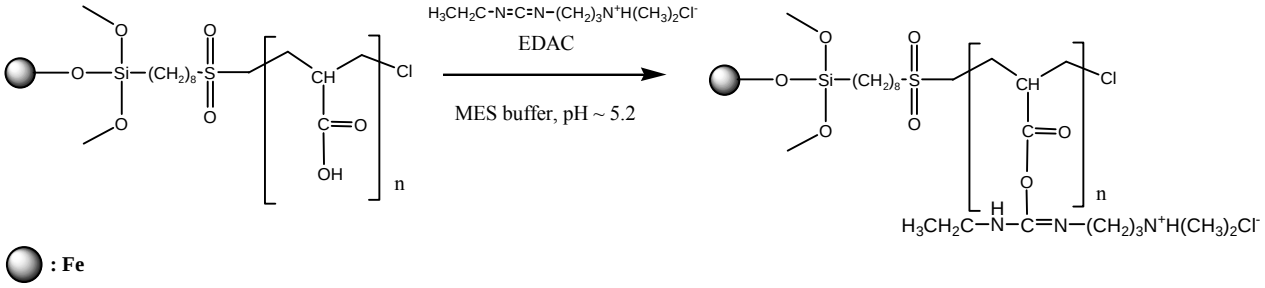

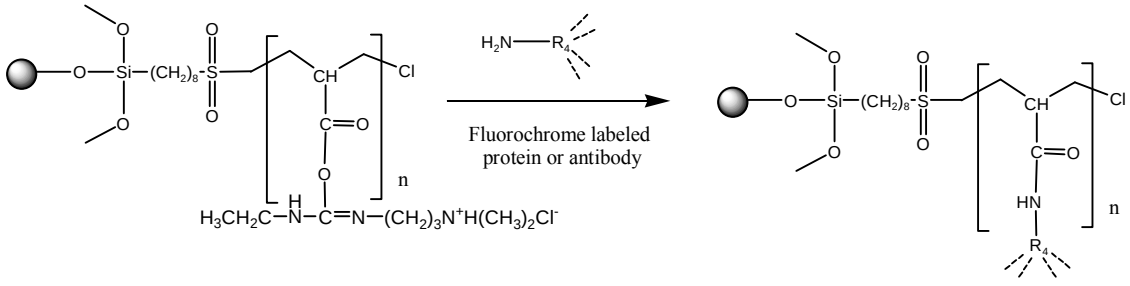

(B)

Figure 13: The conjugation mechanism of Polylink carboxylic acid functionalized microsphere with protein (5).

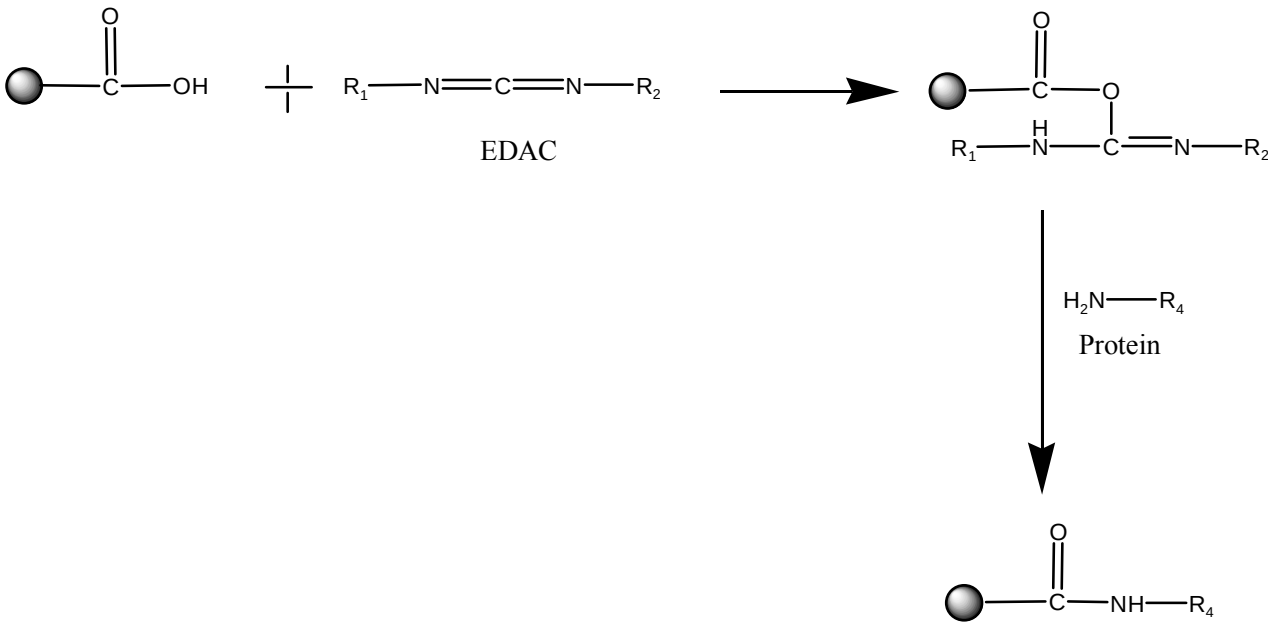

Grafted polymers	Experiment (^{o}C)	Literature (^{o}C)
Poly(NIPAAm)	151.5	135 (9)
Poly(AA)	140.4	110 (10)
Poly(NIPAAm-co-AA)	190.9	170 (11)

Table 1: Tg of grafted polymer and literature.

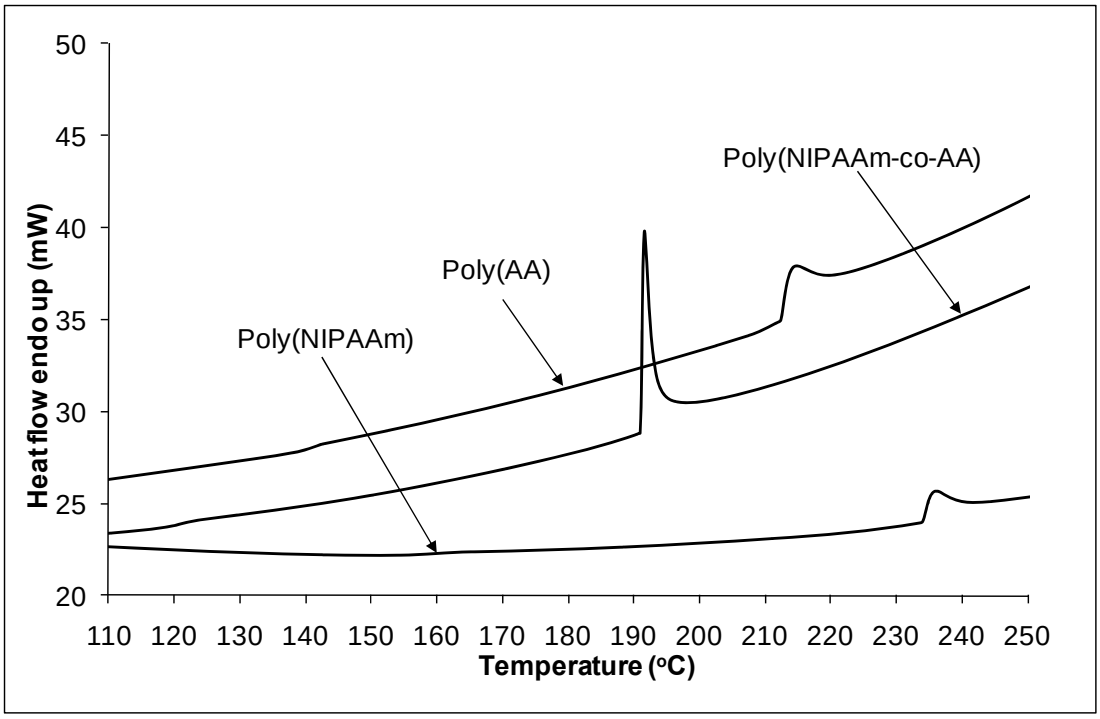

Figure 14: DSC thermograms of various surface grafted polymers.

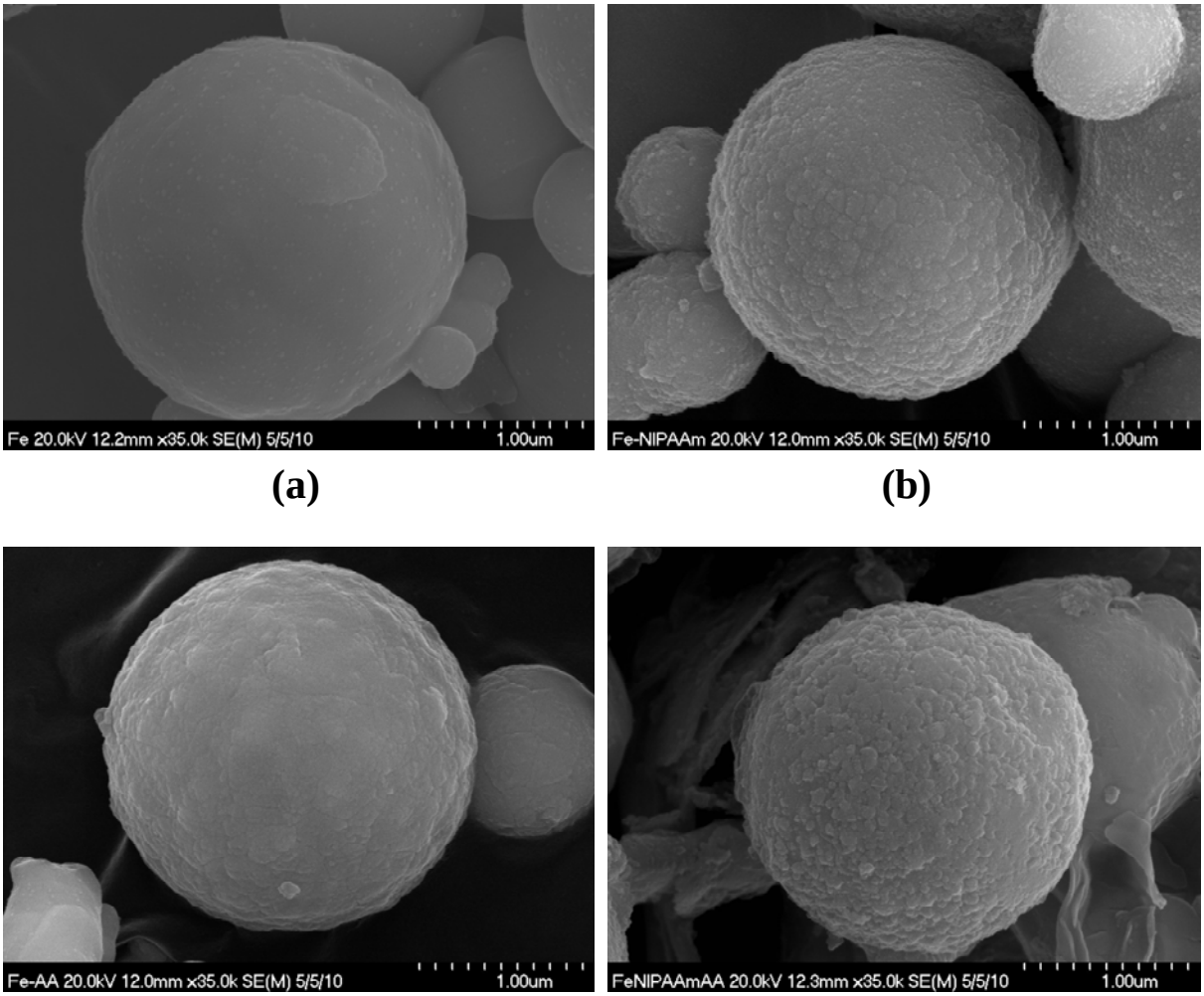

Figure 15: SEM images of iron particles: (a) Non-coated, (b) Poly(NIPAAm) coated, (c) Poly(AA), and (d) Poly(NIPAAm-co-AA).

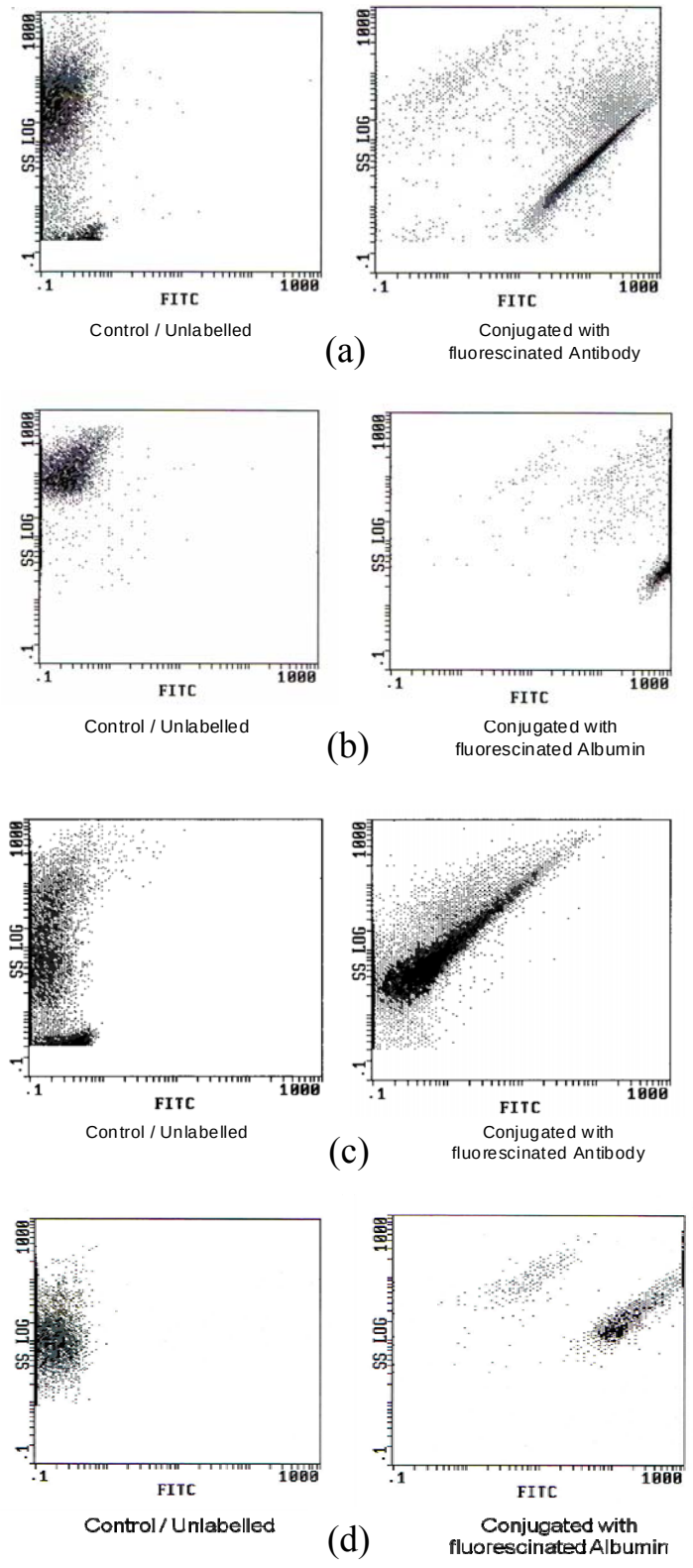

Figure 16: The flow cytometry results of (a) Fe–Poly(AA)– fluorescein (FITC)-conjugated ChromPure Rat IgG, (b) Fe–Poly(AA)–fluorescent labeled albumin, (c) Fe–Poly(NIPAAm-co-AA)–fluorescein (FITC)-conjugated ChromPure Rat IgG, and (d) Commercially carboxylic acid functionalized microsphere with fluorescent labeled albumin.

Figure 17: Thymidine incorporation of in vitro stimulated splenocytes. 3.5 x10^5 splenocytes/ well were stimulated with different concentration of either LPS, anti-CD40 or iron-conjugated-CD40 and incubated at 37°C for 4 days. On day 4 each well was pulsed with 1 µCi [^{3}H] and incubated at 37°C for 16-18hours then plate was harvested on a Wallac-scintillation counter for thymidine incorporation. Each stimulation was done in quadruplet for each concentration of LPS or CD40 or iron-CD40. CPM: counts per minute. Statistics by Two-way ANOVA, *, **, *** versus LPS group and ^ versus iron-CD40 group.